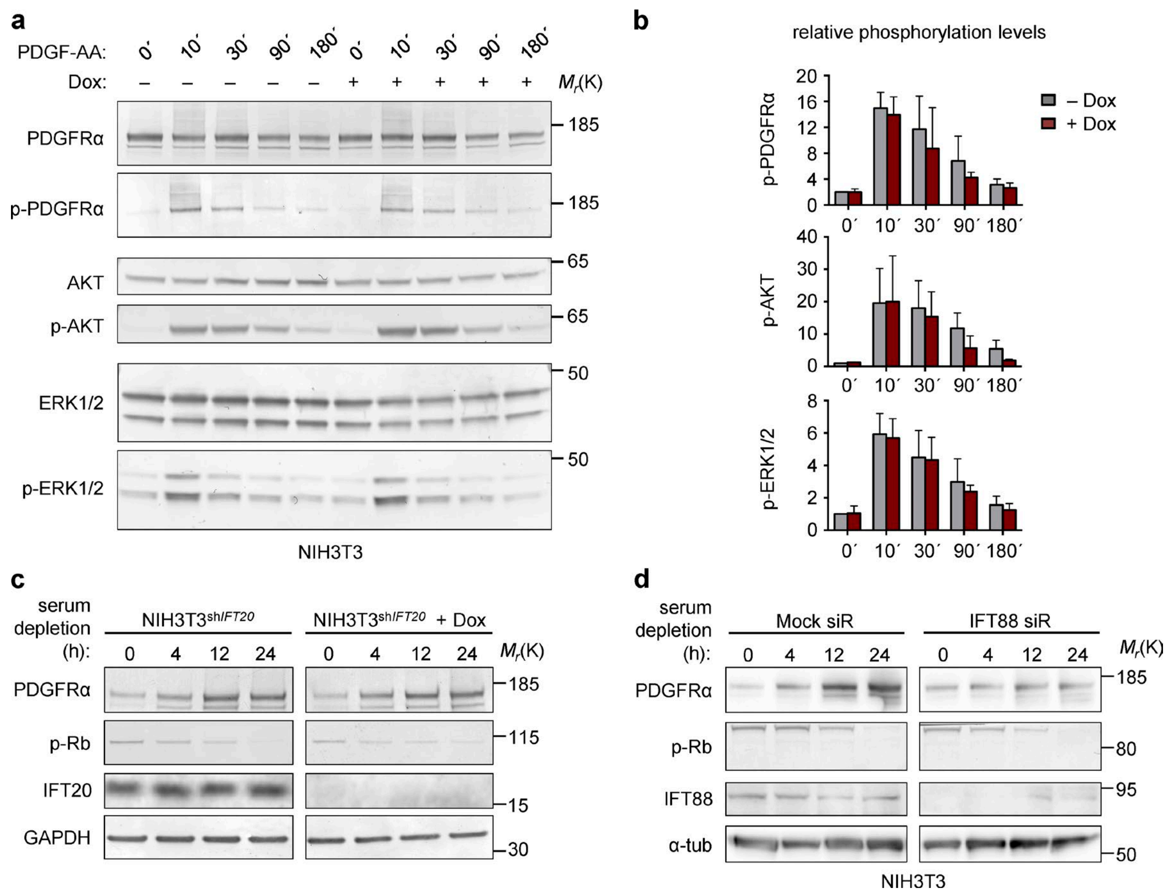

Figure S1. **Dox treatment does not affect PDGFRα signaling in WT NIH3T3 cells, and PDGFRα is up-regulated at the protein level in growth-arrested cells depleted for IFT20. (a)** WB analysis of phosphorylation of PDGFRα (p-PDGFRα), AKT (p-AKT), and ERK1/2 (p-ERK1/2) upon stimulation with PDGF-AA for the indicated times in growth-arrested NIH3T3 cells with or without Dox treatment for 6 d. **(b)** Quantification of protein phosphorylations shown in panel a. Error bars represent means ± SEM (n = 3). **(c)** WB analysis of PDGFRα levels upon serum depletion for indicated times in NIH3T3*shIFT20* cells treated with or without Dox for 6 d. **(d)** WB analysis of PDGFRα levels upon serum depletion for indicated times in NIH3T3 cells with and without siRNA (siR)-mediated silencing of IFT88. Experiments presented in panels c and d were repeated at least three times, and results from representative experiments are shown.

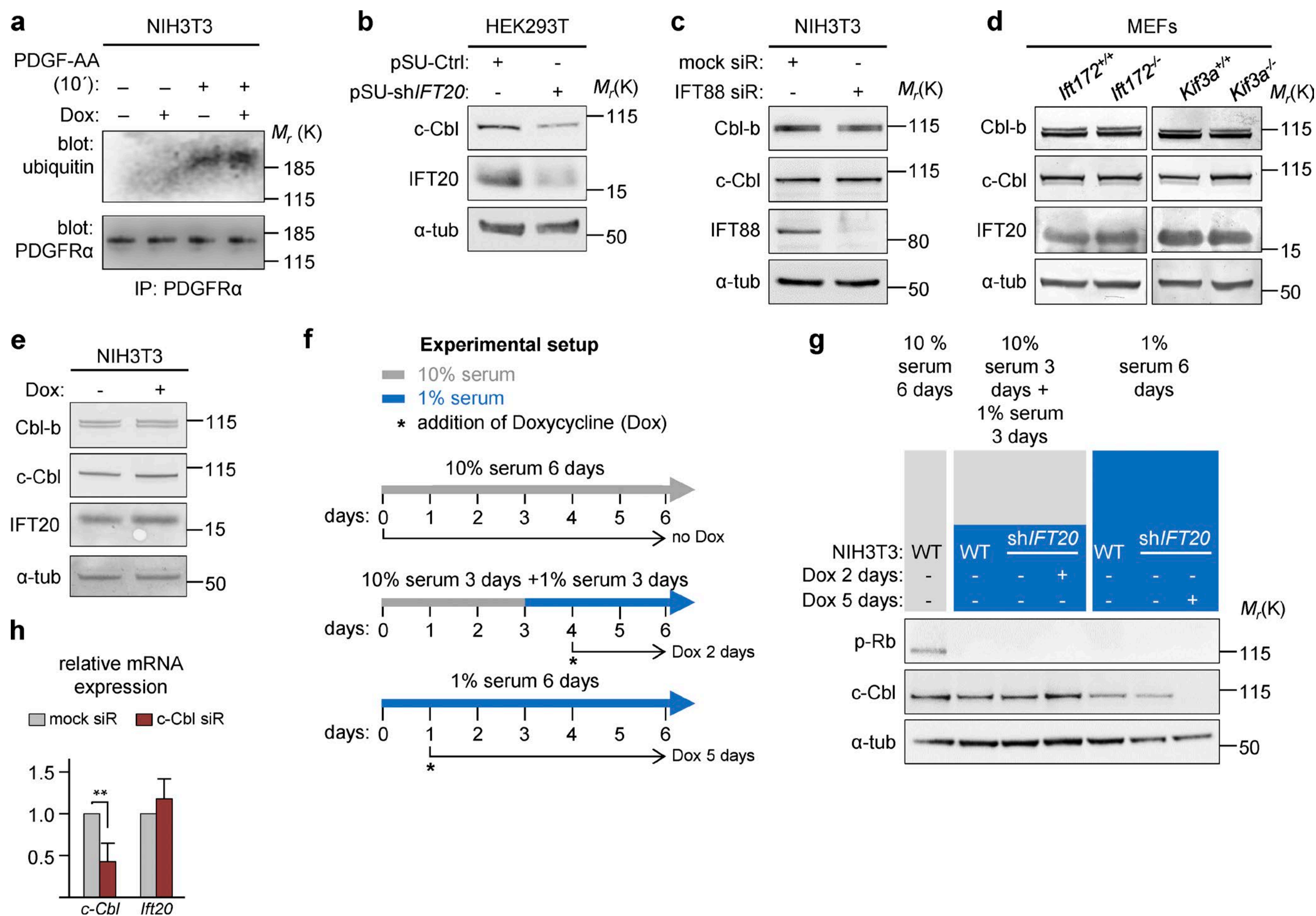

Figure S2. **Instability of c-Cbl in cycling and growth-arrested cells depleted for IFT20. (a)** PDGFRα ubiquitination upon stimulation with PDGF-AA for 10 min in growth-arrested NIH3T3 control cells, with or without Dox treatment for 6 d before ligand addition. IP using anti–PDGFRα; WB analysis using an antibody against mono– and polyubiquitin as well as PDGFRα. **(b)** WB analysis of c-Cbl levels in HEK293T cells transiently transfected with pSuperior vector expressing an shRNA against human IFT20 (pSU-shIFT20) or a control shRNA (pSU-Ctrl). **(c)** WB analysis of Cbl-b and c-Cbl in growth-arrested WT NIH3T3 cells subjected to either mock or siRNA (siR)-mediated silencing of IFT88. **(d)** WB analysis of Cbl-b, c-Cbl, and IFT20 in *Kif3a*$^{-/-}$ and *Ift172*$^{-/-}$ mouse embryonic fibroblasts. **(e)** WB analysis of Cbl-b and c-Cbl in growth-arrested WT NIH3T3 cells with or without Dox for 6 d. **(f)** Graphic illustration of the experimental setup used to obtain results shown in panel g. **(g)** WB analysis of c-Cbl levels in WT NIH3T3 or NIH3T3^{shIFT20} cells cultured in the presence of 1% serum for 24 h (to induce growth arrest) before treatment with Dox for the indicated times. Cells were cultured in 1% serum, because of cell lethality when grown without serum for 6 d. Staining of phosphorylated Rb (p-Rb) marks cycling NIH3T3 cells cultured in the presence of 10% serum. All experiments presented in panels a–e and g were repeated at least three times, and results from representative experiments are shown. **(h)** Quantitative, real-time PCR analysis of relative *Ift20* mRNA transcript levels in NIH3T3 control cells upon 6 d of Dox treatment. Error bars represent means ± SEM (*n* = 3).

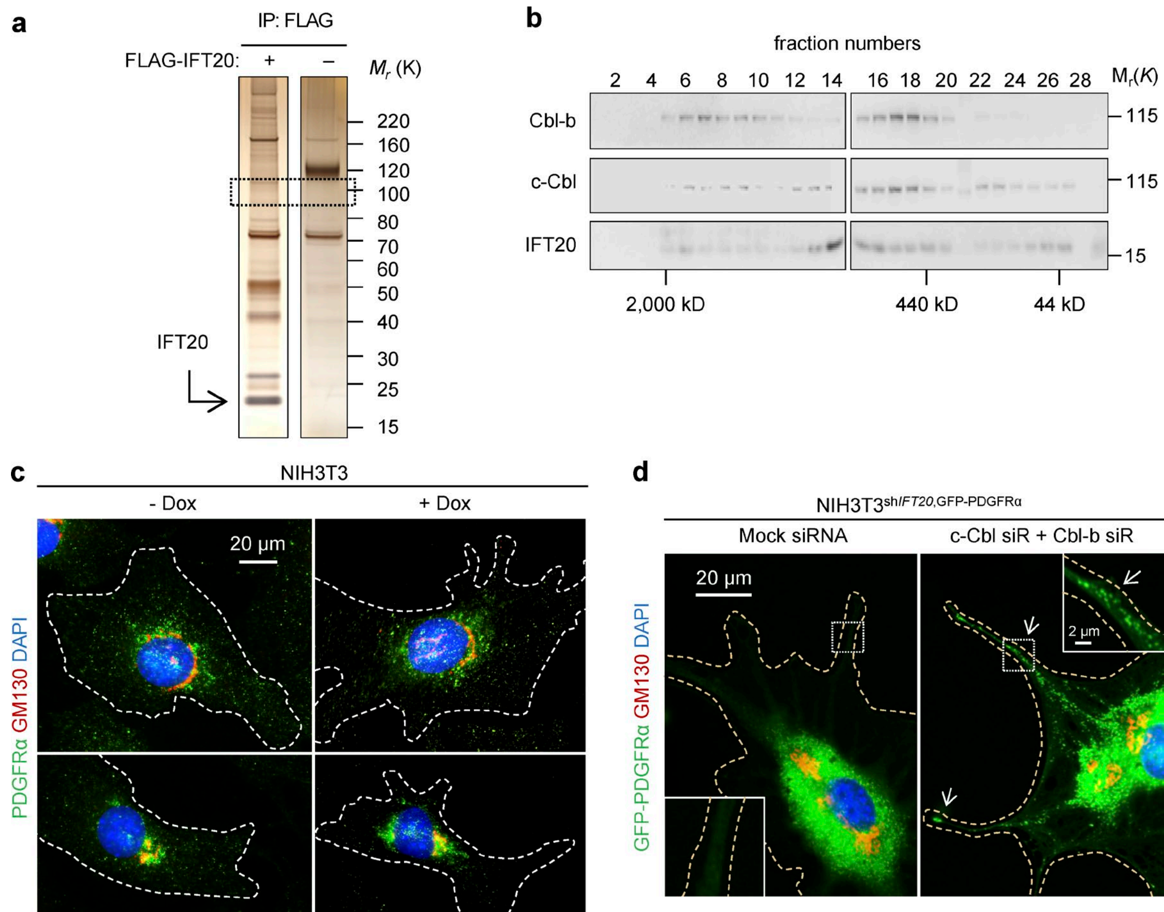

Figure S3. **Interaction between IFT20 and Cbl proteins, ciliary localization of c-Cbl, and mislocalization of PDGFRα in Cbl-depleted cells. (a)** Silver staining of gel containing resolved protein eluates derived from FLAG IP of either FLAG–IFT20 or empty FLAG vector–transfected HEK293T cell extracts. Indicated range shows the gel slices used for mass spectrometric analysis. **(b)** Gel filtration analysis of HEK293T cell extracts. **(c)** IFM analysis of localization of endogenous PDGFRα in NIH3T3 control cells upon 6 d of Dox treatment. Nuclei (Nu) were visualized with DAPI staining. **(d)** IFM analysis of GFP–PDGFRα localization in NIH3T3$^{shIFT20,GFP\text{-}PDGFR\alpha}$ cells subjected to siRNA (siR)-mediated silencing of both c-Cbl and Cbl-b. GM130 labels the Golgi complex. Arrows indicate localization of receptors to cellular protrusions. Nuclei were visualized with DAPI.

Provided online is one table in Excel. Table S1 shows MS-based analysis of proteins interacting with FLAG–IFT20. The list represents the highest scoring number of peptides in the gel slice excised and used in the MS. HEK293T cells were either mock transfected or transfected with FLAG–IFT20 plasmid. FLAG–IFT20 and its associated proteins were enriched using an anti-FLAG–conjugated agarose resin and analyzed by MS. c-Cbl (CBL) is indicated in red.